Atmos. Chem. Phys., 10, 7267–7283, 2010
www.atmos-chem-phys.net/10/7267/2010/
doi:10.5194/acp-10-7267-2010

Atmospheric Chemistry and Physics

The importance of aerosol mixing state and size-resolved composition on CCN concentration and the variation of the importance with atmospheric aging of aerosols

J. Wang[1], **M. J. Cubison**[2], **A. C. Aiken**[2], **J. L. Jimenez**[2], **and D. R. Collins**[3]

[1]Atmospheric Sciences Division, Brookhaven National Laboratory, Upton, NY, USA
[2]Department of Chemistry and Biochemistry, and CIRES, University of Colorado, Boulder, CO, USA
[3]Department of Atmospheric Sciences, Texas A&M University, College Station, TX, USA

Received: 15 April 2010 – Published in Atmos. Chem. Phys. Discuss.: 5 May 2010
Revised: 10 July 2010 – Accepted: 22 July 2010 – Published: 6 August 2010

Abstract. Aerosol microphysics, chemical composition, and CCN concentrations were measured at the T0 urban supersite in Mexico City during Megacity Initiative: Local and Global Research Observations (MILAGRO) in March 2006. The aerosol size distribution and composition often showed strong diurnal variation associated with traffic emissions and aging of aerosols through coagulation and local photochemical production of secondary aerosol species. CCN concentrations (N_{CCN}) are derived using Köhler theory from the measured aerosol size distribution and various simplified aerosol mixing state and chemical composition, and are compared to concurrent measurements at five supersaturations ranging from 0.11% to 0.35%. The influence of assumed mixing state on calculated N_{CCN} is examined using both aerosols observed during MILAGRO and representative aerosol types. The results indicate that while ambient aerosols often consist of particles with a wide range of compositions at a given size, N_{CCN} may be derived within ∼20% assuming an internal mixture (i.e., particles at a given size are mixtures of all participating species, and have the identical composition) if great majority of particles has an overall κ (hygroscopicity parameter) value greater than 0.1. For a non-hygroscopic particle with a diameter of 100 nm, a 3 nm coating of sulfate or nitrate is sufficient to increase its κ from 0 to 0.1. The measurements during MILAGRO suggest that the mixing of non-hygroscopic primary organic aerosol (POA) and black carbon (BC) particles with photochemically produced hygroscopic species and thereby the increase of their κ to 0.1 take place in a few hours during daytime. This rapid process suggests that during daytime, a few tens of kilometers away for POA and BC sources, N_{CCN} may be derived with sufficient accuracy by assuming an internal mixture, and using bulk chemical composition. The rapid mixing also indicates that, at least for very active photochemical environments such as Mexico City, the timescale during daytime for the conversion of hydrophobic POA and BC to hydrophilic particles is substantially shorter than the 1–2 days used in some global models. The conversion time scale is substantially longer during night. Most POA and BC particles emitted during evening hours likely remain non-hygroscopic until efficiently internally mixed with secondary species in the next morning. The results also suggest that the assumed mixing state strongly impacts calculated N_{CCN} only when POA and BC represent a large fraction of the total aerosol volume. One of the implications is that while physically unrealistic, external mixtures, which are used in many global models, may also sufficiently predict N_{CCN} for aged aerosol, as the contribution of non-hygroscopic POA and BC to overall aerosol volume is often substantially reduced due to the condensation of secondary species.

Correspondence to: J. Wang
(jian@bnl.gov)

1 Introduction

Atmospheric aerosols affect the global energy budget by scattering and absorbing sunlight (direct effects) and by changing the microphysical structure, lifetime, and coverage of clouds (indirect effects). An increase in aerosol concentration would lead to smaller cloud droplet size and higher cloud albedo, i.e., brighter clouds (Twomey, 1977). This effect, which is known as the first indirect aerosol effect, tends to cool the global climate. The smaller cloud droplet size resulting from increased aerosol concentration also inhibits

precipitation, leading to an increase in cloud lifetime and coverage (second indirect aerosol effect; Albrecht, 1989). Although it is widely accepted that the indirect effects can strongly influence the global climate, and potentially mask the warming effect due to anthropogenic CO_2, the magnitudes of indirect aerosol effects are poorly understood. The Intergovernmental Panel on Climate Change (IPCC, 2007) considers the indirect effects of aerosols the most uncertain components in forcing of climate change over the industrial period.

Among the key challenges in quantifying the aerosol indirect effects is to determine the spectrum of cloud condensation nuclei (CCN) and its spatial and temporal variations. CCN are particles that can grow into cloud droplets at atmospherically relevant water supersaturations. For particles consisting of inorganic compounds, CCN activity can be effectively predicted using Köhler theory (Köhler, 1936) based on physicochemical properties of the solute, such as its mass, molecular weight, density, and activity coefficient. As ambient particles are often comprised of substantial amounts of organic species (Kanakidou et al., 2005; Murphy et al., 2006; Zhang et al., 2007), Köhler theory has been extended to include the influence of organic species on surface tension (Facchini et al., 1999) and their contributions as solute (Shulman et al., 1996). Laboratory studies have shown that CCN activities of single- and some multi-component aerosols can be successfully described using the extended Köhler theory (Raymond and Pandis, 2002, 2003; Bilde and Svenningsson, 2004; Huff-Hartz et al., 2006; Svenningsson et al., 2006). Once the size distribution, size-resolved composition, and mixing state of aerosols are known, the CCN concentrations may be accurately predicted by applying the extended Köhler theory. However, detailed information on composition and mixing state is often not available or incomplete for ambient aerosols, partially due to the limitation of current measurement techniques and the lack of routine measurements. Ambient aerosols are often complex mixtures of both inorganic and organic components, and their composition can vary substantially with particle size. In addition, for a given size, particles may range from consisting mainly of a single species to mixtures of multiple components with a wide spectrum of proportions. In extreme cases, a complete and rigorous description of aerosol composition and mixing state may require information on each individual particle, which is beyond current measurement capabilities and may not be necessary for many applications. In addition, given the computational constraints, the representation of aerosol composition and mixing state in large scale models (e.g., GCM and CTM) are often greatly simplified. The description of aerosol composition ranges from bulk (i.e., size independent) composition (e.g., Ming et al., 2007), to modal and bin representations that take into consideration the variation in chemical composition between modes or size bins (Gong et al., 2003; Easter et al., 2004; Textor et al., 2006). Some models consider aerosol to be an internal mixture (i.e., at any size, particles are mixtures of all participating species and have the identical composition, this definition of internal mixture will be used throughout this study), and many models assume an external mixture, (i.e., aerosol contains types of particles consisting of a single species, and the number fraction of each particle type is determined by the aerosol composition, this definition will be used throughout this study) (Textor et al., 2006). These two approaches represent simplifications of the complex mixing states of ambient aerosols, but can be considered as the two extreme scenarios of the aerosol mixing state.

Given the limitation of current measurement techniques and the computational constraint in large scale models, it is important to understand the uncertainty in calculated CCN concentration (N_{CCN}) due to these simplified representations of aerosol mixing state and composition. Aerosol mixing state also controls the influence of other aerosol parameters on predicted N_{CCN}. For example, for internally mixed aerosols, predicted N_{CCN} is often insensitive to the hygroscopicity of organics as the CCN activation is largely determined by highly-hygroscopic inorganic species (e.g. Chang et al., 2007; Prenni et al., 2007; Wang et al, 2008). While it is generally accepted that N_{CCN} strongly depends on particle size distribution (e.g., Dusek et al., 2006, Ervens et al., 2007), currently there is no consensus on how much detail on aerosol mixing state and chemical composition is needed to sufficiently predict N_{CCN}. For prediction of N_{CCN}, the applicability of either internal or external mixture, which is widely used in global models, is expected to vary among aerosol types and with the aging of atmospheric aerosols. CCN concentration was found to be predicted with sufficient accuracy assuming simplified composition and an internal mixture in some studies (e.g. Liu et al., 1996; Cantrell et al., 2001; Roberts et al., 2002; VanReken et al., 2003, Rissler et al., 2004; Conant et al., 2004; Gasparini et al., 2006; Ervens et al., 2007; Chang et al., 2007; Andreae and Rosenfeld 2008; Wang et al. 2008, Gunthe et al., 2009; Rose et al., 2008a; Shinozuka et al., 2009), whereas other studies suggest prediction of N_{CCN} may require detailed chemical composition, mixing state, and/or the properties of organics being taken into consideration (e.g., Mircea et al., 2005; Broekhuizen et al., 2006; Mochida et al., 2006; Stroud et al., 2007; Cubison et al., 2008; Quinn et al., 2008). Medina et al. (2007) find a $\sim$35% overprediction of N_{CCN} for semi-urban air masses in New Hampshire even when size-resolved aerosol composition is employed, and attribute the overprediction to the assumption of an internal mixture. Sensitivity studies on measurements at the Duke Forest site in North Carolina show calculated N_{CCN} was highly sensitive to the assumed aerosol mixing state, but lack of mixing state measurements preclude a quantitative evaluation of its effect on closure (Stroud et al., 2007). A realistic treatment of mixing state of urban aerosols is also found to be critical to eliminate significant biases in calculated N_{CCN} in Cubison et al. (2008). Ervens et al. (2010) study the impact of the assumed mixing state and

composition on calculated N_{CCN} and find that detailed chemical composition (size-resolved) and mixing state are often required for predicting N_{CCN} for aerosols close to pollution sources. Within a few tens of kilometers downwind of emission sources, N_{CCN} could be reproduced within a factor 2 by assuming either externally or internally mixed, hygroscopic organics.

In this study, the influences of aerosol mixing state and size-resolved chemical composition on predicted N_{CCN} and the variations of the influences with aerosol aging are examined using data collected at an urban site during the Megacity Initiative: Local and Global Research Observations (MILAGRO) study. CCN concentrations are calculated from the measured aerosol size distributions and various simplified scenarios of aerosol mixing state and chemical composition using Köhler theory. The calculated N_{CCN} are then compared to concurrent measurements at five supersaturations ranging from 0.11% to 0.35%. The closure agreement between measurement and calculation based on various simplifications and the variation of the closure agreement with the aging of the aerosol are examined. The influence of assumed mixing state on predicted N_{CCN} is studied using both aerosols observed during MILAGRO and representative aerosol types. The implications of the results on simplified representations of aerosol for sufficiently predicting N_{CCN} and cloud microphysics in large scale models are discussed.

2 Measurements

2.1 Location

The data used here were collected during the MILAGRO study (Molina et al., 2010) at the T0 supersite, which was located at the Instituto Mexicano del Petroleo (IMP, 19°29′23″N, 99°08′55″W, 2240 m altitude, ∼780 mbar ambient pressure), 9 km NNE of the center of Mexico City, near a combination of residential, commercial and light industrial areas. The closest street with significant road traffic was 200 m from the site. Data presented in this study include aerosol size distribution, CCN spectra, mixing state, and chemical composition, all of which were measured from the top of a building, ∼28 m above ground level, from 10 to 31 March 2006. Except for measured and calculated N_{CCN}, which are reported at standard temperature and pressure (STP, 1013.25 hpa and 273.15 K), all other measurements are reported at local ambient pressure and temperature conditions. Local time (UTC minus 6 h) is used throughout this study. The individual measurements and instruments are described in the following sections.

2.2 Aerosol size distribution

Aerosol size distribution was measured by a Scanning Mobility Particle Sizer (SMPS) (Wang et al., 2003). The major components of the SMPS are a cylindrical Differential Mobility Analyzer (Model 3081, TSI Inc., Minneapolis, MN) and a Condensation Particle Counter (Model 3010, TSI Inc., Minneapolis, MN). Aerosol size distribution ranging from 15 nm to ∼560 nm was measured with a temporal resolution of 2 min. The relative humidity (RH) of the SMPS sample flow was always below 30% during MILAGRO, and was below 25% for vast majority of the size distribution measurements, suggesting sampled aerosol particles were effectively dry. The SMPS was calibrated using polystyrene latex standards. Data from the SMPS were reduced using the data inversion procedure described by Collins et al. (2002).

2.3 CCN concentrations

CCN concentrations were measured by a CCN counter (Droplet Measurement Technologies, Boulder, CO; Roberts and Nenes, 2005). Prior to MILAGRO, the DMT CCN counter was calibrated at the T0 site using ammonium sulfate, with sample temperature (measured at the first temperature control stage) of 27.6 °C, a flow rate of 0.3 L min^{-1}, and longitudinal temperature gradients of 6.0, 7.0, 8.0, 10.0, 12.0 °C. Based on this calibration, the supersaturations (S) derived from Köhler theory using a constant van't Hoff factor of 2.5 are 0.11%, 0.17%, 0.22%, 0.29%, and 0.35% for the five temperature gradients. This supersaturation range of 0.11–0.35% is within the typical range of climatically important marine stratocumulus clouds. During MILAGRO, the flow rates were maintained the same as during the calibration, and the temperature gradient was stepped through the 5 values every 36 min. Measurements made before temperatures had stabilized following changes of the temperature gradient are excluded from analysis. As the calibration was carried out at the T0 site (i.e. at the same sampling pressure), pressure correction for instrument supersaturations is not necessary. During MILAGRO, the CCN sample temperature varied from 24 to 32 °C, i.e., 4 °C below and above the sample temperature during the calibration. Such variation in sample temperature leads to an uncertainty of ∼6% (relative) in instrument supersaturation (Rose et al., 2008b), which is well within the uncertainty of calibrations. Therefore, the small influence of sample temperature on instrument supersaturation is neglected in our analysis.

2.4 Aerosol hygroscopic growth factor distribution and mixing state

The size-resolved aerosol hygroscopicity, from which aerosol mixing state is inferred, was measured by a Tandem Differential Mobility Analyzer (TDMA) system (Gasparini et al., 2004). In the TDMA, the classifying voltage of the first DMA is held constant to select a monodisperse aerosol of dry diameter D_p^*. This monodisperse aerosol is then exposed to an actively controlled RH of 85%, and the size distribution of the humidified aerosol is measured by the

second DMA, in which the classifying voltage is scanned, and a downstream condensation particle counter (CPC). The response of the aerosol to increased RH is quantified by the hygroscopic growth factor, which is defined as the ratio of the diameter of a particle at an elevated RH (i.e., 85% in this study) to its dry diameter D_p^* (RH<20%). The aerosol mixing state is inferred from the growth factor distribution as discussed below. Hygroscopic growth factor distributions were measured at 7 dry diameters (12, 25, 50, 100, 200, 300, and 400 nm). The measurements at all 7 dry diameters required approximately 40 min to complete. The TDMA was coupled to a specialized CCN instrument during much of the MILAGRO campaign. Consequently, of the 941 measurement sequences completed during the study, only 387 were the ambient aerosol measurements used in this analysis.

2.5 Aerosol chemical composition

An Aerodyne high-resolution aerosol mass spectrometer (HR-AMS; DeCarlo et al., 2006; Canagaratna et al., 2007) was also deployed at T0, and reported the composition (bulk and size resolved) for non-refractory submicron particles. The HR-AMS reported size distribution for chemical species vs. vacuum aerodynamic diameter (D_{va}; DeCarlo et al., 2004), from which volume equivalent diameter (D_{ve}) was estimated assuming sphericity and using the estimated size-resolved density (as discussed below). The instrumental intercomparisons and main results of the HR-AMS in this study have been reported in previous publications (Aiken et al., 2008, 2009, 2010; Paredes-Miranda et al., 2009; Huffman et al., 2009; Salcedo et al., 2010; Cappa and Jimenez, 2010)

The AMS reported non-refractory inorganic species (sulfate, nitrate, ammonium, and chloride) as well as total organic aerosol (OA). The OA measured by the AMS was classified into different components using Positive Matrix Factorization (Paatero, 1997; Ulbrich et al., 2009) of the high-resolution OA spectra, as described by Aiken et al. (2009). For the purposes of the CCN analyses in this paper the size-resolved OA was classified into two factors. The first factor is hydrocarbon-like organic aerosol (HOA) which is considered a surrogate of primary OA (POA) from urban combustion sources. The size distribution of HOA was calculated from the estimated size-distribution of the $C_4H_9^+$ fragment which is generally dominated by HOA (Aiken et al., 2009; Zhang et al., 2005a). The size distribution of the second OA factor was estimated as the difference between those of total OA and HOA. The second OA factor consists mainly of oxygenated organic aerosols (OOA), a surrogate for secondary OA, and biomass burning organic aerosols (BBOA) (Aiken et al., 2009). This second factor is referred to as O+BBOA in this study. Classification of the size-resolved OA into more factors is limited by the limited signal-to-noise of the size-resolved data. In addition, previous studies show BBOA and SOA have similar hygroscopicity (King et al., 2007; Petters and Kreidenweis, 2007; Vestin et al., 2007; Andreae and Rosenfeld, 2008; Carrico et al., 2008; Asa-Awuku et al., 2009; King et al., 2009; Gunthe et al., 2009), therefore we do not expect that grouping OOA and BBOA together will introduce substantial biases in calculated N_{CCN}.

Black carbon (BC) mass concentration was estimated from measured light absorption using a seven-channel aethalometer at T0 during MILAGRO (Marley et al., 2009), which compared well with collocated instruments (Paredes-Miranda et al., 2009). The cut size for the sampling line was 2 μm. Black carbon is a strongly absorbing component whose light absorption coefficient has weaker spectral dependence than those of some absorbing organic material and dust. The mass concentration of BC is derived from absorption measurements at 880 nm and 950 nm, at which aerosol absorption is dominated by BC (Marley et al., 2009). The BC size distribution was estimated from the size distribution of HOA and then normalized to the bulk BC mass (Zhang et al., 2005b; Cubison et al., 2008).

3 Data overview: diurnal variation of aerosols observed at T0 during MILAGRO

Strong diurnal variations in aerosol properties were observed at the T0 site during MILAGRO. Aerosol size distribution, mass concentration of aerosol species, hygroscopic growth factor distribution for particles with dry diameter of 100 nm, and CCN concentration (N_{CCN}) at 0.22% supersaturation are averaged for the weekdays, and their diurnal variations are shown in Fig. 1a–d (all data presented in this study are from weekdays, when clear diurnal cycles of aerosol properties were observed). The distributions of hygroscopic growth factor ($d\overline{N}/d\log_{10}\left(D_p/D_p^*\right)$ where $\overline{N}$ is the normalized number concentration) exhibit similar diurnal variations for particles with initial dry diameters of 50, 100, and 200 nm, which encompass the typical range of particle critical activation diameter (D_{pc}, the minimum diameter of CCN at a given supersaturation) at the 5 sampled supersaturations. From 06:00 to 08:00, high concentrations of Aitken mode particles were often observed, which are associated with fresh traffic emission during morning hours. This is consistent with elevated concentrations of BC and HOA. The distribution of particle hygroscopic growth factor is bimodal, with the dominant peak at $D_p/D_p^* = 1$. This suggests that non-hygroscopic BC and POA from traffic emissions represent a large fraction of the Aitken mode particles, and are externally mixed with particles containing hygroscopic species, which represent the second mode of growth factor at $\sim$ 1.5. Starting from $\sim$07:30 a.m., substantial increases in nitrate and O+BBOA concentrations were observed, and are attributed to photochemical productions of nitrate and SOA (Sunrise ranged from 06:32 to 06:49 during MILAGRO in Mexico City), as described for Mexico City in multiple recent publications (e.g. Salcedo et al., 2006; Volkamer et al., 2006;

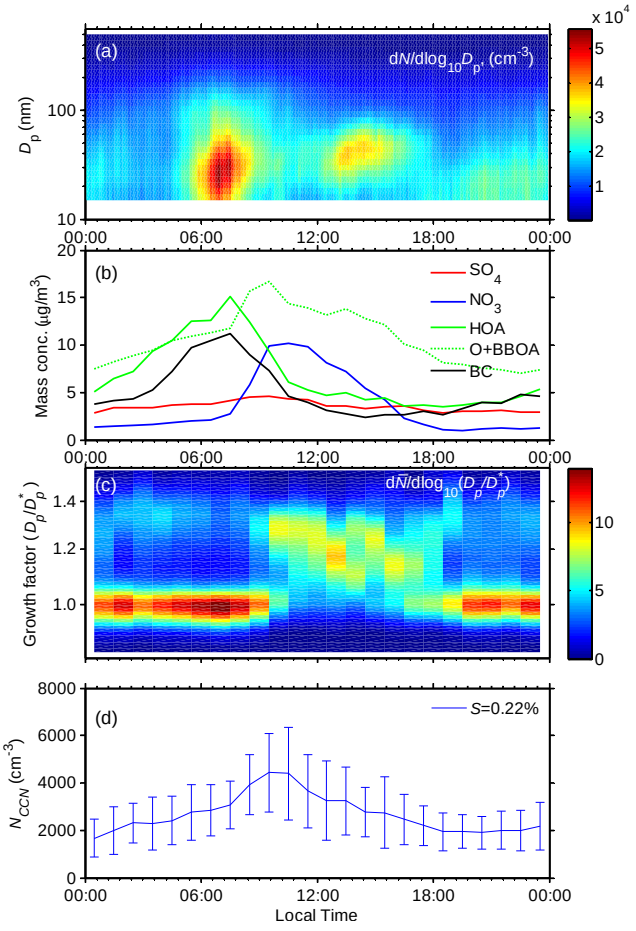

Fig. 1. Diurnal variations of aerosol properties observed at the T0 site during weekdays. **(a)** Aerosol size distribution measured by SMPS; **(b)** Mass concentrations of SO_4, NO_3, hydrocarbon-like organic aerosol (HOA), oxygenated organic aerosol and biomass burning organic aerosol (O+BBOA), and black carbon (BC); **(c)** Hygroscopic growth factor distribution at 85% RH for 100 nm dry particles; **(d)** Mean and standard deviation of N_{CCN} measured at 0.22% supersaturation.

Paredes-Miranda et al., 2009; Dzepina et al., 2009; Cross et al., 2009). The elevated concentration of nitrate, a highly hygroscopic species, is likely the main reason for the increased N_{CCN} (Fig. 1d). Within a few hours from 09:00 to 12:00, the dominant non-hygroscopic mode disappeared, and the distribution of hygroscopic growth factor changed from bimodal to unimodal, suggesting non-hygroscopic HOA and BC particles were quickly coated by secondary hygroscopic species, including nitrate and SOA. The absence of the non-hygroscopic HOA and BC particles was also partially due to the dilution by the rapidly rising boundary layer. The unimodal distribution of growth factor is quite broad, suggesting particles with a wide spectrum of compositions. Starting from ~18:00, increases in Aitken mode particle number concentration, BC and HOA mass concentration were again observed, and are associated with evening traffic emissions. These evening increases were less pronounced compared to those observed in morning hours, likely due to somewhat lower emission rates and slightly more mixing in the evening (Velasco et al., 2009). As expected, the growth factor distribution indicates non-hygroscopic BC and HOA were externally mixed with other species during the evening hours. A large fraction of the BC and HOA remained externally mixed through the night, because coagulation, the main mechanism to mix BC and HOA with other hygroscopic species in the absence of photochemistry, is less effective than the condensation of secondary hygroscopic species during daytime (Riemer et al., 2004). Consistent conclusions have been reached from the analysis of single-particle mass spectrometry data from MILAGRO (Moffet et al., 2008; Cross et al., 2009).

4 Methods

4.1 Derivation of chemical composition and mixing state from measurements

Aerosol chemical composition, required to calculate N_{CCN} at the five supersaturations, is derived from the AMS and aethalometer measurements using the following approach. In this study, the aerosol species considered include SO_4^{2-}, NO_3^-, NH_4^+, HOA, O+BBOA, and BC. Soil and Cl^- are neglected as they had negligible (less than 5% by mass combined, Aiken et al., 2009) contribution to particles ranging from 50 to 200 nm, the typical range of the D_{pc} at the five measured supersaturations. SO_4^{2-} and NO_3^- were fully neutralized during MILAGRO (Aiken et al., 2009). Therefore, aerosols are assumed to consist of five species: $(NH_4)_2SO_4$, NH_4NO_3, BC, HOA, and O+BBOA. AMS and aethalometer measurements are averaged into 1-h intervals to increase signal-to-noise ratio (SNR). This averaging is especially necessary for size resolved mass concentrations from AMS because of the limited SNR arising from the low duty cycle during size-resolved measurements. At each size, species volume fractions, required to calculate overall hygroscopicity of multi-component particles, are derived from mass concentrations and densities of participating species. The densities of $(NH_4)_2SO_4$ and NH_4NO_3 are assumed to be 1770 kg m^{-3} and 1730 kg m^{-3}, respectively. A density of 1770 kg m^{-3} is used for BC (Park et al., 2004). Organics are assumed to have a density of 1250 kg m^{-3}, which is within the typical range of previous measurements (Turpin and Lim, 2001; Cross et al., 2007; Malloy et al., 2009). In derivation of size-resolved composition and N_{CCN}, the particle vacuum aerodynamic diameter (D_{va}, measured by AMS) and particle mobility diameter (D_m, measured by SMPS) are converted to particle volume equivalent diameter (D_{ve}) assuming spherical particles (For spherical particles, both D_m and D_{ve} are equal to particle geometric diameter). This assumption is reasonable

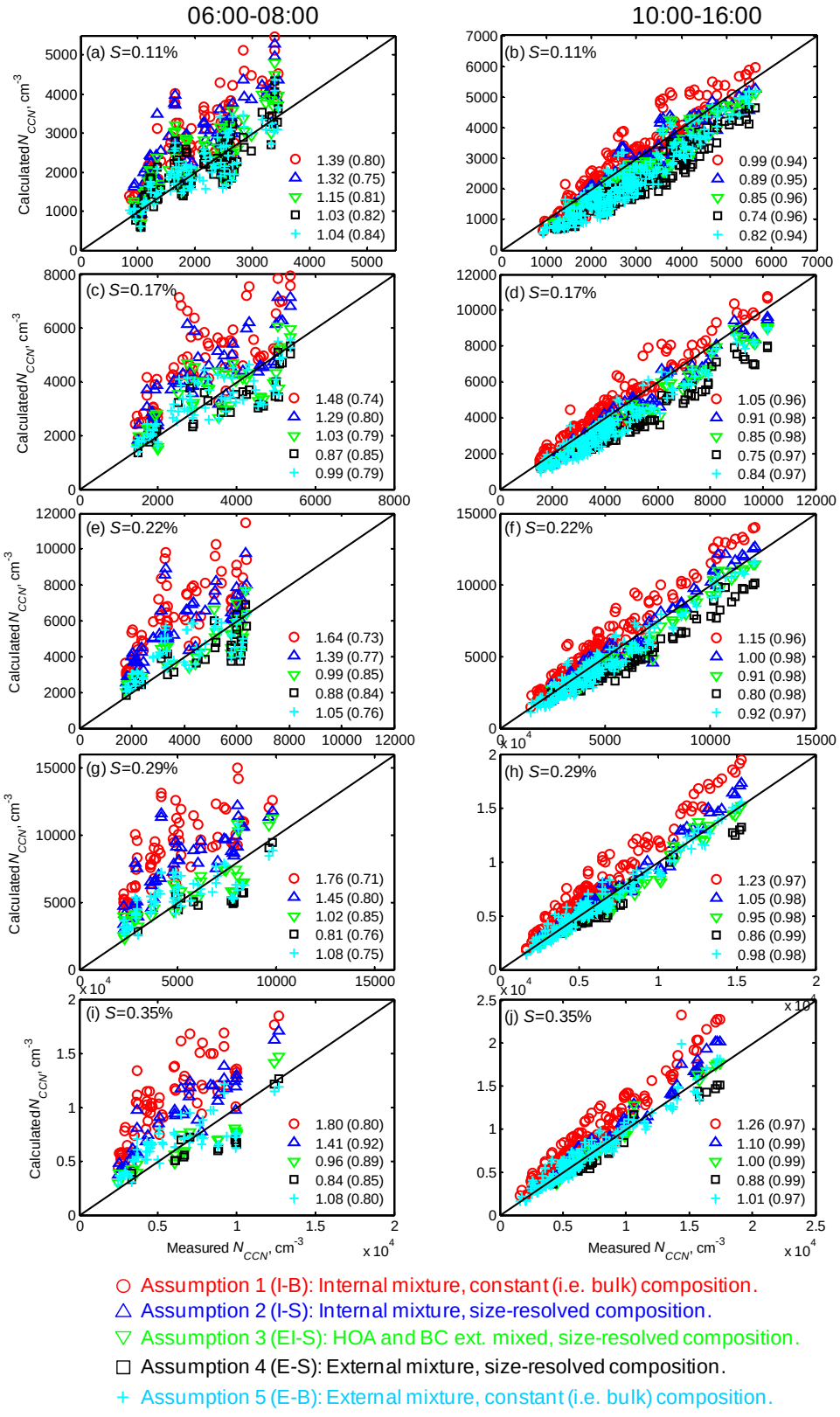

Fig. 2. Comparison of N_{CCN} calculated using five different assumptions and the measurements at supersaturations of 0.11% (**a** and **b**), 0.17% (**c** and **d**), 0.22% (**e** and **f**), 0.29% (**g** and **h**), and 0.35% (**i** and **j**) for periods of 06:00–08:00 (a, c, e, g, and i) and 10:00–16:00 (b, d, f, h, and j). The slope (left) and the correlation coefficient (r, in the parenthesis) are shown for all assumptions on each plot.

except for freshly emitted, externally mixed BC particles, which are non-spherical aggregates of individual spherules produced by combustion. For fresh BC particles, the assumption of spherical particles leads to overestimate of D_{ve} from D_m and underestimate of D_{ve} from D_{va} (DeCarlo et al., 2004). Without the information on BC morphology and its variation with particle size and time, it is difficult to estimate the influence of this assumption on calculated N_{CCN}. To examine the importance of the mixing state and the chemical composition, five different assumptions are applied to calculate N_{CCN} at the five supersaturations.

Assumption 1: internal mixture with size independent (i.e., bulk) composition (I-B)

In this assumption, sub-micrometer particles are treated as internal mixtures, and all particles have the identical (i.e., average) chemical composition for the entire sub-micrometer size range. The average composition is derived from bulk mass concentration of species measured by the AMS and aethalometer.

Assumption 2: size resolved composition with internal mixture at each size (I-S)

At each particle size, the aerosol is considered internally mixed and particles have the identical composition; however the particle composition (i.e., species volume fractions), and therefore the overall hygroscopicity of particles, vary across the sub-micrometer size range. The particle composition at each size is derived from mass size distribution of the five species described earlier.

Assumption 3: size resolved chemical composition with sulfate, nitrate, O+BBOA internally mixed at each size, and BC and HOA externally mixed at each size (EI-S)

At each particle size, $(NH_4)_2SO_4$, NH_4NO_3, and O+BBOA are internally mixed, while HOA and BC are externally mixed. In this assumption, there are three distinct types of particles at any given size: BC particles, HOA particles, and secondary-dominated particles (internal mixtures of $(NH_4)_2SO_4$, NH_4NO_3, and O+BBOA). As detailed later, HOA and BC are assumed to be non-hygroscopic, therefore only the mixture consisting of $(NH_4)_2SO_4$, NH_4NO_3, and O+BBOA can serve as CCN under the measured supersaturation. The composition of the internally mixed particle varies with particle size, and is derived from mass size distributions. At each particle size, the number concentration of the internally mixed particles is calculated as the product of total particle concentration (i.e., measured by SMPS) and the number fraction, which is derived as the sum of the volume fractions of $(NH_4)_2SO_4$, NH_4NO_3, and O+BBOOA. (The average size-resolved composition during MILAGRO is shown in Figs. 2b–c of Aiken et al., 2009).

Assumption 4: external mixture with size dependent composition (E-S)

In this assumption, sub-micrometer aerosol species are treated as externally mixed. At each size, there are five different types of particles, each composed of a single species. The number concentration of each type of particles is calculated as the product of the total particle number concentration and the number (volume) fraction of the species. The particle composition, and therefore the number fraction of each type of particle, vary with particle diameter and are derived from the mass size distribution and density of the species.

Assumption 5: external mixture with size independent composition (E-B)

Same as assumption 4 (i.e., E-S), except that aerosol has the same (i.e. average) composition, therefore the same number fraction of each particle type, for the entire sub-micrometer size range. The composition is derived from the species bulk mass concentrations. While neither this assumption nor assumption E-S is atmospherically realistic, they are used as the opposite extremes of the assumptions I-B and I-S, and allow us to examine the impact of mixing state on calculated N_{CCN}. In addition, aerosols are often assumed to be external mixtures in global models (Textor et al., 2006).

4.2 κ-Köhler theory and calculation of CCN concentrations

In this study, the critical dry diameter that corresponds to activation at supersaturations inside the CCN counter was calculated using "κ-Köhler theory" (Petters and Kreidenweis, 2007), which employs a single parameter κ to describe the Raoult effect on CCN activation. In κ-Köhler theory, the water vapor saturation ratio over the aqueous solution droplet S is given by:

$$S = \frac{D^3 - D_p^3}{D^3 - D_p^3(1-\kappa)} \exp\left(\frac{4\sigma_w M_w}{RT\rho_w D}\right) \quad (1)$$

where D is the droplet diameter, D_p the dry diameter of the particle, M_w the molecular weight of water, σ_w the surface tension of pure water, ρ_w the density of water, R the gas constant, T the absolute temperature. For particles comprised of multiple components, the value of κ is given by a simple mixing rule (Petters and Kreidenweis, 2007):

$$\kappa = \sum_i x_i \kappa_i \quad (2)$$

where x is the volume fraction and subscript i denotes species i. For soluble inorganic species, such as $(NH_4)_2SO_4$, NH_4NO_3, κ_i can be derived as:

$$\kappa_i = \nu_i \frac{\rho_i M_w}{\rho_w M_i} \quad (3)$$

where ρ is the density, M the molecular weight, and ν the van't Hoff factor. The van't Hoff factor takes into consideration the non-idealities of water activity, and the values used in study are 2.5 and 1.9 for $(NH_4)_2SO4$, and NH_4NO_3, respectively (Clegg et al., 1998, Petters and Kreidenweis 2007). BC is assumed to be non-hygroscopic and with a κ of zero. The value of κ for aerosol organics ranges from zero for insoluble species to $\sim$0.25 for dicarboxylic acids often observed in SOA. In this study, HOA, representing the primary

OA (POA), is assumed to be non-hygroscopic (i.e., κ =0). O+BBOA, which includes mainly contributions from SOA and BBOA, is assumed to have a κ of 0.15, which is within the typical range observed from environmental smog chamber and field measurements (King et al., 2007; Petters and Kreidenweis 2007; Vestin et al., 2007; Andreae and Rosenfeld 2008; Carrico et al., 2008; Asa-Awuku et al., 2009; King et al., 2009, Gunthe et al., 2009; Petters et al., 2009). For each assumption of aerosol mixing state and chemical composition, critical dry particle activation diameters (D_{pc}) are derived using κ-Köhler theory for the particle types, and N_{CCN} is then derived from the D_{pc} and size distributions measured by the SMPS.

5 Results

5.1 CCN closure study and the sensitivity of calculated N_{CCN} to assumed aerosol mixing state and composition

Figures 2 and 3 show the comparison of calculated and measured N_{CCN} and its variation with local time for the five supersaturations ranging from 0.11% to 0.35%. CCN concentrations calculated using the five assumptions are compared to measurements during the periods of 06:00–08:00 (i.e., morning traffic hours) and 10:00–16:00 (after substantial secondary species were produced through photochemical reactions) on weekdays. Our analyses and discussion are focused on these two periods to contrast the impacts of aerosol mixing state and chemical composition on calculated N_{CCN} for these two well-defined extremes of the composition/mixing state phase space. In addition, high aerosol loadings during these two periods provide better signal-to-noise ratio for the AMS size distributions. The ratio of calculated to measured N_{CCN} is derived through a bivariate least squares fit (i.e., Orthogonal distance regression) and is shown for the two periods in Fig. 2. In addition, the ratio of calculated to measured N_{CCN} is also derived for each hour during weekdays and its variation from 4:00 to 18:00 is presented in Fig. 3. From 06:00 to 08:00, the calculated N_{CCN} is sensitive to assumed aerosol mixing state and chemical composition, especially at the higher supersaturations sampled. At S = 0.35%, there is over a factor of 2 difference (ratio ranging from 0.84 to 1.80) for N_{CCN} calculated using the five different assumptions. The bimodal hygroscopic growth distribution from the TDMA measurements suggests aerosol mixing state and composition during morning traffic hours are best approximated by assumption EI-S, in which freshly emitted hydrophobic POA and BC were externally mixed with other hygroscopic species including nitrate, sulfate and O+BBOA, and size resolved composition is employed. N_{CCN} calculated using assumption EI-S indeed agrees with the measurement very well, with the ratio of calculated to measured N_{CCN} ranging from 0.96 to 1.15 for the period of 06:00–08:00. Assuming aerosol to be an internal mixture (i.e., assumption I-S, with size resolved composition) overestimates N_{CCN} by 29 to 45%. This is because during morning traffic hours, freshly emitted HOA and BC particles, most of which are within the Aitken mode, do not contribute to N_{CCN} at the supersaturations studied. The assumption of internal mixture allows a large fraction of the HOA and BC particles to serve as CCN due to mixing with hygroscopic species, and therefore leads to an overestimate of N_{CCN}. Using the bulk (assumption I-B) instead of the size-resolved composition results in further overestimation. AMS measurements show aerosol volume was dominated by particles with diameter greater than

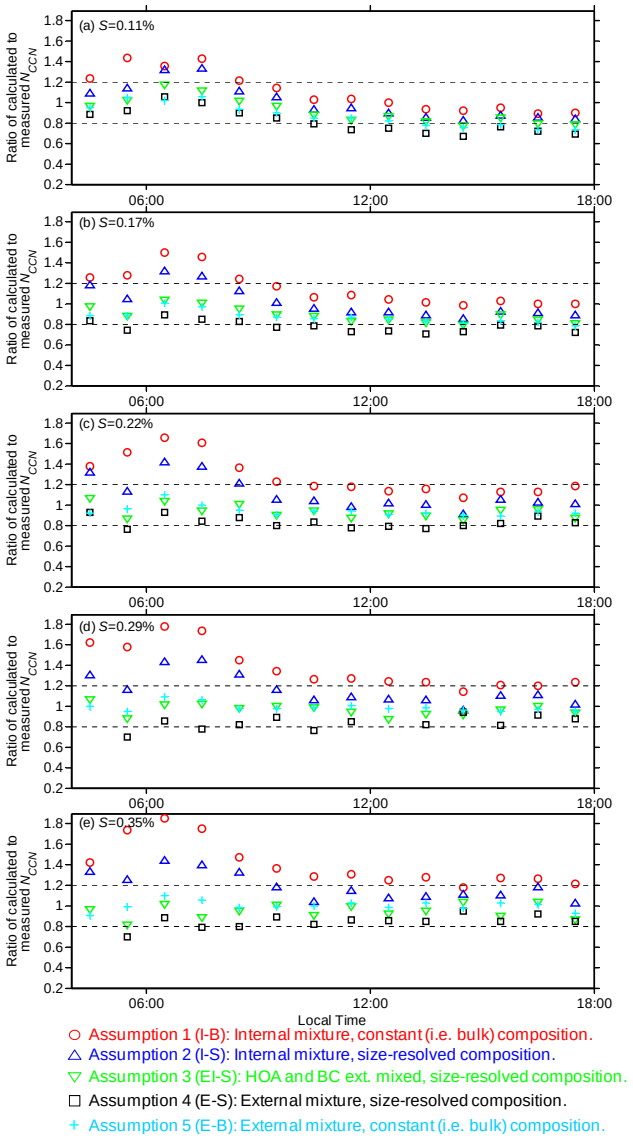

Fig. 3. Variation of the ratio of calculated to measured N_{CCN} at supersaturations of **(a)** 0.11%, **(b)** 0.17%, **(c)** 0.22%, **(d)** 0.29%, and **(e)** 0.35% as a function of local time and assumptions on aerosol mixing state and composition.

200 nm. The bulk composition reflected the composition of particles around 200 to 400 nm, which are greater than the D_{pc} at the five supersaturations. As the volume fractions of highly hygroscopic sulfate and nitrate mostly increased with particle diameter from 50 nm to 400 nm at the T0 site, using the bulk composition leads to positive biases in volume fraction of nitrate and sulfate, and thereby κ of internally mixed particles near D_{pc}, which results in an underestimate of D_{pc} and further overestimation of N_{CCN}. As D_{pc} increases with decreasing supersaturation, this additional overestimate arising from using the bulk composition is less pronounced at lower supersaturations, as bulk composition better represents the composition at the larger D_{pc}. The additional overestimate can be represented by the difference in the ratio between assumptions I-B and I-S, which increases from 7% (i.e. 1.39–1.32) to 39% (1.80–1.41) as S increases from 0.11 to 0.35%. Overall, the overestimate when using assumption I-B increases from 39% to 80% when S increases from 0.11% to 0.35%.

When the aerosol is assumed to be an external mixture and size-resolved composition is used (assumption E-S), the calculated N_{CCN} is underestimated by less than 20% for the five supersaturations during 06:00–08:00. It is worth noting that when N_{CCN} is calculated using assumption E-B, the underestimate due to the assumption of external mixture is offset by the overestimate arising from the use of bulk concentration, and the ratio of calculated to measured N_{CCN} is very close to 1, ranging from 0.99 to 1.08. Overall, the impact of aerosol mixing state and composition on calculated N_{CCN} decreases with decreasing supersaturation, partially because using bulk composition introduces less bias for large D_{pc} at lower supersaturations. The ratio of calculated to measured N_{CCN} ranges from 0.84 to 1.80 at $S = 0.35\%$, and this range is reduced to from 1.03 to 1.39 at $S = 0.11\%$.

From 08:00 to 12:00, the non-hygroscopic mode from the TDMA measurements quickly subsided. The distribution of hygroscopic growth changed from bimodal to unimodal, indicating the freshly emitted HOA and BC were rapidly mixed with other hygroscopic species. This fast transition is attributed mainly to coating of HOA and BC particles by photochemically-produced SOA and ammonium nitrate, which show rapid increases in concentration during this period, together with dilution of the morning traffic particles in the rapidly rising boundary layer. This is consistent with earlier modeling studies that show condensation of secondary hygroscopic species is the dominant pathway in converting hydrophobic BC into hydrophilic particles (Riemer et al., 2004, 2009). The N_{CCN} calculated using assumption I-S, which best approximates the observed aerosol mixing state and composition during this period, agrees with measurements well for all supersaturations, and the ratio of calculated to measured N_{CCN} ranges from 0.89 to 1.10 for the five supersaturations. We note that the broad unimodal distribution of the growth factor distribution suggests particles with a wide range of compositions, and the assumption of an internal mixture (i.e., identical composition at each particle size) is a great simplification of the actual aerosol mixing state. The implication of this simplification will be further discussed in the next section. In a few hours, the ratios of calculated to measured N_{CCN} using different assumptions quickly converge to around unity (Fig. 3). Compared to that during morning traffic hours, the calculated N_{CCN} during 10:00–16:00 is much less sensitive to the assumption of aerosol mixing state and chemical composition applied. The contrast is most pronounced for $S = 0.35\%$, when the difference among N_{CCN} calculated using different assumptions is reduced from over a factor 2 (i.e., ratio ranging from 0.84 to 1.8) during morning traffic hours to ~40% (i.e., ratio ranging from 0.88 to 1.26). There also appears to be much less scatter in the comparison of calculated and measured N_{CCN} during 10:00–16:00, as evidenced from the high correlation coefficients. The above results suggest that for urban aerosols such as those observed at T0 site, N_{CCN} may be calculated assuming an internal mixture and using bulk composition a few hours after particles are emitted, or a few tens of kilometers away from the source.

From 18:00 to 24:00 and 00:00 to 04:00, a persistent non-hygroscopic mode from the TDMA measurements suggests most HOA and BC particles emitted during evening traffic hours remain externally mixed throughout the night (Fig. 1c). This persistent non-hygroscopic mode also suggests that condensation of photochemically produced species is the dominant pathway for mixing HOA and BC with hygroscopic species. As the aerosol mass, and therefore the SNR of the AMS size-distributions, were relatively low during this period, N_{CCN} are calculated using bulk composition from the AMS (not shown in Fig. 2). When the aerosol is assumed to be an internal mixture and the bulk concentration is used (assumption I-B), the calculated N_{CCN} also shows similar positive bias, although somewhat smaller than that during the morning traffic hours. At $S = 0.35\%$, using assumption I-B results in an overestimate of N_{CCN} by 44% during the period from 18:00 to 4:00, compared to 80% from 06:00 to 08:00.

The impact of assumed aerosol mixing state and composition on calculated N_{CCN} is examined by comparing the ratio of calculated to the measured N_{CCN}, denoted by r, under different assumptions. The difference between N_{CCN} calculated using various assumptions is estimated from $(r_X - r_Y)/r_Y$ (where subscripts X and Y represent different assumptions) for the two periods of 06:00–08:00 and 10:00–16:00; the results are given in Table 1. Table 1 shows that $(r_{I-S} - r_{EI-S})/r_{EI-S}$, which represents the difference between assumptions of internally and externally mixed HOA and BC, is much greater for the period of 06:00–08:00 than that during 10:00–16:00, especially at high supersaturations. At $S = 0.35\%$, $(r_{I-S} - r_{EI-S})/r_{EI-S}$ is 47% during 06:00–08:00, compared to 10% for the period of 10:00–16:00. Between the two periods, $(r_{I-B} - r_{I-S})/r_{I-S}$, representing the overestimate due to using the bulk composition for an internal mixture, generally exhibits slightly higher values during

Table 1. Relative differences between N_{CCN} calculated using various assumptions (estimated using $\frac{r_X - r_Y}{r_Y}$, where subscripts X and Y represent different assumptions) for the periods of 06:00–08:00 and 10:00–16:00 on weekdays.

S(%)	$(r_{I-B}$-$r_{I-S})/r_{I-S}$ (%)*		$(r_{I-S}$-$r_{EI-S})/r_{EI-S}$ (%)†		$(r_{EI-S}$-$r_{E-S})/r_{E-S}$ (%)‡		$(r_{E-S}$-$r_{E-B})/r_{E-B}$ (%)#	
	06:00–08:00	10:00–16:00	**06:00–08:00**	**10:00–16:00**	06:00–08:00	10:00–16:00	06:00–08:00	10:00–16:00
0.11	5	11	**15**	**5**	12	15	−1	−10
0.17	15	15	**25**	**7**	18	13	−12	−11
0.22	18	15	**40**	**10**	13	14	−16	−13
0.29	21	17	**42**	**11**	26	10	−25	−12
0.35	28	15	**47**	**10**	14	14	−22	−13

* Overestimate due to using the bulk composition for an internal mixture.
† Difference between the assumptions of internally and externally mixed HOA and BC.
‡ Difference between the assumptions of internally and externally mixed nitrate, sulfate, and O+BBOA.
# Difference between using size-resolved and bulk compositions for an external mixture.

the period of 06:00–08:00. Similarly, the difference between using size-resolved and bulk compositions for the external mixtures (represented by $(r_{E-S} - r_{E-I})/r_{E-I}$) is also somewhat greater during 06:00–08:00. These suggest that during 10:00–16:00, particle composition became more homogeneous among different sizes, therefore using bulk composition leads to less bias in derived N_{CCN}. Table 1 also shows that $(r_{EI-S} - r_{E-S})/r_{E-S}$, representing the difference between the assumptions of internally and externally mixed nitrate, sulfate, and O+BBOA, are comparable for the two periods, and mostly within 20%. These comparisons suggest that the large differences in N_{CCN} calculated using various assumptions for the period of 06:00–08:00 are largely due to different assumptions of the mixing state of non-hygroscopic HOA and BC, which are further examined in the next section.

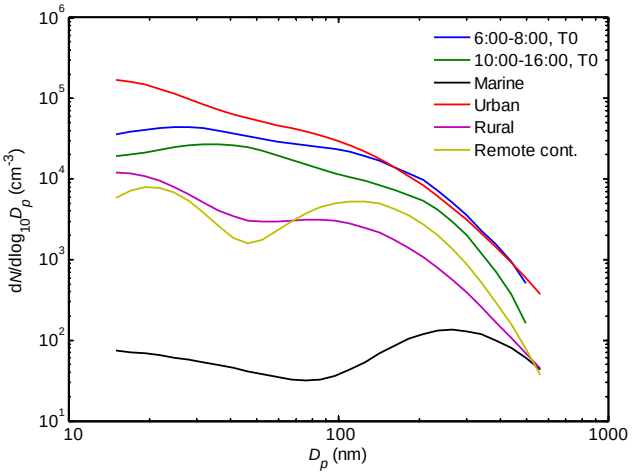

Fig. 4. Size distributions averaged over the periods of 08:00–10:00 and 10:00–16:00 at the T0 site during MILAGRO weekdays, and size distributions of typical marine, urban, rural, and remote continental aerosols.

5.2 Impact of mixing state on calculated N_{CCN} and its variation with aerosol aging

To examine the importance of assumed aerosol mixing state on calculated N_{CCN} and the variation of the importance with aerosol aging, a sensitivity study is carried out using aerosols with a variety of size distributions and compositions. The analysis includes aerosol size distributions averaged over the period of 08:00–10:00 and 10:00–16:00 at T0 during MILAGRO weekdays, as well as those of representative aerosol types, including typical marine, urban, rural, and remote continental aerosols (Seinfeld and Pandis, 2006). The aerosol size distributions are shown in Fig. 4. For each aerosol type, particles are assumed to consist of organics (representing non-hygroscopic or weakly hygroscopic species) and sulfate (representing highly hygroscopic inorganic salts). The volume fraction of organics is assumed independent of particle size and varies among 20%, 50%, and 80%, which encompass the typical range of organic volume fraction in ambient aerosols. The relative difference between N_{CCN} calculated assuming internal and external mixtures are represented by $(N_{CCN,int} - N_{CCN,ext})/N_{CCN,int}$, which is shown as a function of κ of organics (κ_{org}) for the supersaturations of 0.1, 0.15, 0.2., 0.3, and 0.4% (Fig. 5). Here, $N_{CCN,int}$ and $N_{CCN,ext}$ are CCN concentrations calculated assuming internal and external mixtures of sulfate and organics, respectively.

As expected, $(N_{CCN,int} - N_{CCN,ext})/N_{CCN,int}$ often reaches its highest value at κ_{org} =0, when the difference between the hygroscopicities of two participating species (i.e., organics and sulfate) is the greatest. The relative difference in calculated N_{CCN} generally decreases with increasing κ_{org}. For each aerosol size distribution and composition, the relative difference, $(N_{CCN,int} - N_{CCN,ext})/N_{CCN,int}$, strongly depends on the supersaturation. For aerosols observed during 06:00–08:00, and typical urban, continental, and rural aerosols, the difference is generally lower at lower supersaturations, and is mostly less than 20% at $S = 0.1\%$.

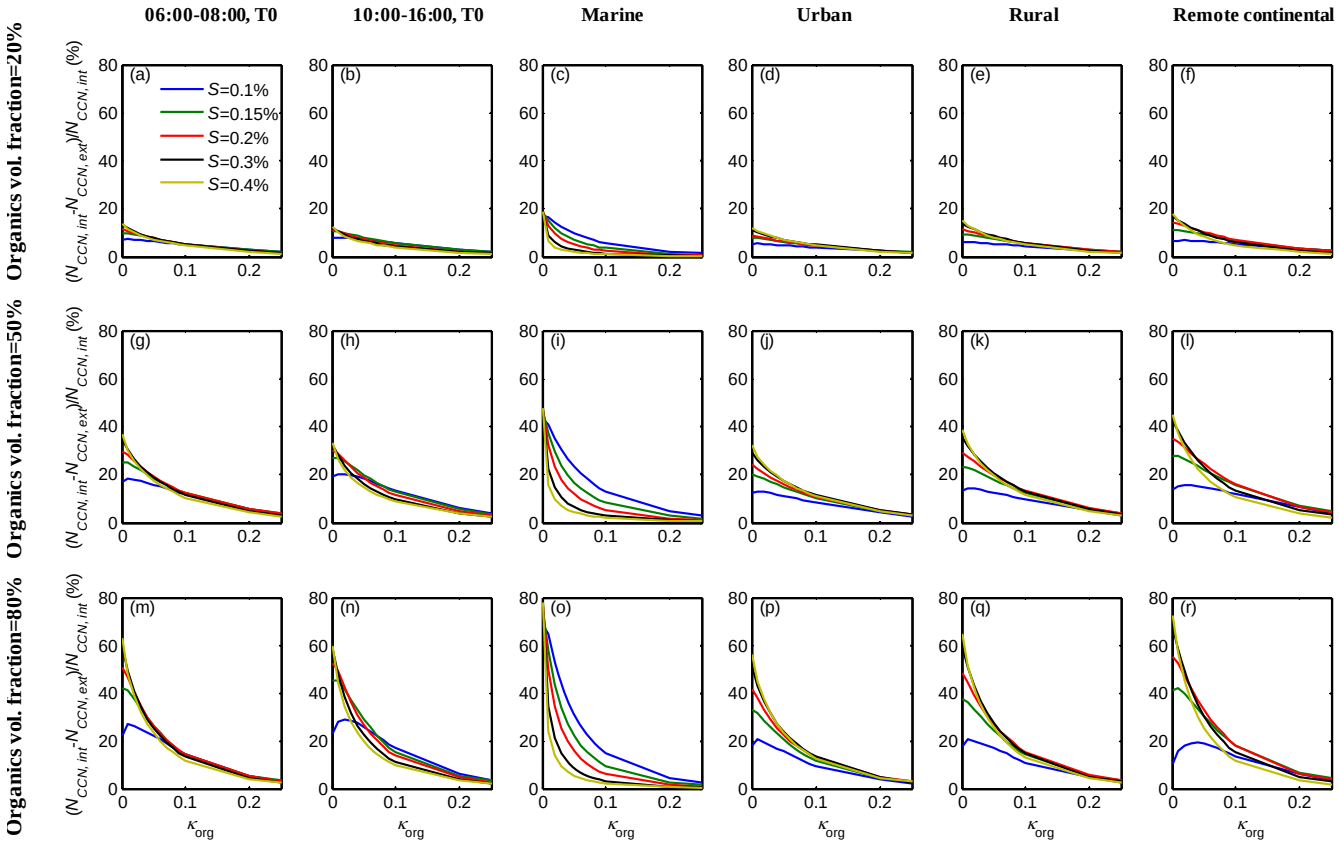

Fig. 5. Relative differences between N_{CCN} calculated with assumptions of internal and external mixtures as a function of κ_{org}. The difference is calculated at supersaturations of 0.1, 0.15, 0.2, 0.3, 0.4% for size distributions averaged during 06:00–08:00 **(a, g, m)** and 10:00–16:00 **(b, h, n)** during MILAGRO weekdays, and size distributions of typical marine **(c, i, o)**, urban **(d, j, p)**, rural **(e, k, q)**, and remote continental **(f, l, r)** aerosols with organic volume fractions of 20% (a, b, c, d, e, f), 50% (g, h, i, j, k, l), and 80% (m, n, o, p, q, r).

In contrast, for aerosols observed during 10:00–16:00 and typical marine aerosols, the difference is greater at lower supersaturations in most of the κ_{org} range.

The relative difference also increases with increasing volume fraction of organics, which represents non-hygroscopic or weakly-hygroscopic species in this sensitivity study. When organics contribute to only 20% of the total aerosol volume, the maximum difference (occurs at $\kappa_{org} = \sim 0$) is less than 16% for all cases. The difference reaches 70% at $\kappa_{org} = 0$ when the organic volume fraction increases to 80%. The relative difference $\left(N_{CCN,int} - N_{CCN,ext}\right)/N_{CCN,int}$ decreases rapidly as the κ_{org} increases, especially at supersaturations greater than 0.2%. In nearly all cases, the difference is less than 20% when κ_{org} exceeds 0.1, and less than ~10% when κ_{org} is greater than 0.15, suggesting that mixing state plays a minor role if all aerosol species have κ greater than 0.1. This is because at a given supersaturation, D_{pc} for species with κ greater than 0.10 are often sufficiently close. For example, at 0.3% supersaturation, the D_{pc} for sulfate, which has a κ of 0.61 and represents highly hygroscopic species in ambient aerosols, is about 63 nm, whereas the D_{pc} for species (e.g. organics) with κ of 0.1 is about 114 nm. Despite the apparent large difference (i.e., a factor of 6) in their κ values, the manifestation of the difference in D_{pc} is rather modest (i.e., less than a factor of 2 in D_{pc}). As sulfate, nitrate, SOA, and BBOA all typically have κ values of ~0.1 or greater (King et al., 2007; Petters and Kreidenweis 2007; Vestin et al., 2007; Andreae and Rosenfeld 2008; Carrico et al., 2008; Asa-Awuku et al., 2009; King et al., 2009; Gunthe et al., 2009), the above results suggest that assumed mixing state strongly impacts calculated N_{CCN} only when POA and BC represent a large fraction of the total aerosol volume. This finding is consistent with results from the T0 site presented earlier, which show large differences among calculated N_{CCN} using different mixing states during morning traffic hours, when HOA and BC represented 52% of the total aerosol volume. A much reduced difference among calculated N_{CCN} is found during 10:00–16:00, when HOA and BC only represent 23% of the total aerosol volume.

The assumptions of internal and external mixtures represent great simplifications of the mixing state of ambient particles. At any given size, ambient particles often have a wide spectrum of chemical compositions, ranging from consisting mainly of a single species to complex mixtures with variety

of compositions. Observational and modeling studies suggest that after some atmospheric processing, most species are to some degree mixed within particles. This is not in the sense that particles at a give size have the identical species mass fractions (i.e., internal mixture assumptions used in this study), but that most particles consist of a variety of hygroscopic and non-hygroscopic species, with a distribution of mass fractions at each size. The TDMA measurements from 10:00–16:00 are consistent with this picture: the unimodal growth factor distribution is broad and indicates mixed particles with a wide range of compositions. Results from the above sensitivity analyses suggest that if great majority of particles has an overall κ value greater than 0.1 (instead of individual species in the above discussion), N_{CCN} can then be calculated within ~20% assuming an internal mixture. This corresponds to less than ~10% in the uncertainty of derived droplet number concentration (Sotiropoulou et al., 2006). One of the important pathways to convert particles from hydrophobic to hydrophilic is through condensation of secondary species, including sulfate, nitrate, and SOA. Increasing the overall κ of a non-hygroscopic particle from 0 to 0.1 corresponds to a volume fraction of condensed sulfate (or nitrate) of 16% ($0.61 \times 16\% = 0.1$). For a non-hygroscopic particle with 100 nm diameter, this translates into a thin sulfate coating of 3 nm thickness. For a coating thickness of 5 nm, the overall κ of the particle (with original diameter of 100 nm) is greater than 0.15, and N_{CCN} can be calculated within ~10% assuming an internal mixture. During MILAGRO, the measurements at T0 site suggest that during daytime, the mixing of freshly emitted POA and BC particles with other hygroscopic species takes place in a few hours, owing to the rapid formation and condensation of secondary nitrate and SOA. This rapid transition was also observed from single-particle mass spectrometry data taken at the T0 site (Moffet et al., 2009), and in an earlier microscopy study in Mexico City (Johnson et al., 2005). By 12:00 p.m., most particles have growth factors greater than 1.16 at 85% RH, which corresponds to an overall κ value of 0.1. This is consistent with the earlier results that show that despite the broad range of particle composition (as evidenced by the range in growth factor), N_{CCN} during 10:00–16:00 are calculated with sufficient accuracy (within ~ 20%) assuming internal mixtures. Once the overall κ of a particle is greater than 0.1, it may readily serve as CCN at atmospheric relevant supersaturations. Therefore, the rapid mixing of POA and BC with other hygroscopic species also suggests a substantially shorter time scale during daytime for converting hydrophobic species into hydrophilic particles than the 1-2 days used in many global models (Wilson et al., 2001; Chung and Seinfeld, 2002; Textor et al., 2006), at least for photochemically active areas. In contrast, the persistent non-hygroscopic mode from the TDMA measurements indicate a much longer (estimated at least 8 hours) time scale at night due to the lack of photochemical production of secondary hygroscopic species. This suggests that the aging timescale should be linked to the production of secondary hygroscopic species, which, to the first order, may be estimated from the product of the concentrations of OH and precursors.

5.3 Comparison to aging time scales from previous studies

Some earlier studies show somewhat longer photochemical time scales, ~12 h, for the aging of BC particles (Moteki et al., 2007; Shiraiwa et al., 2007). Besides the differences in concentrations of gas phase precursors and meteorological conditions, the difference in the derived time scales may largely be due to the different criteria used to define the aging of BC particles. Using SP2 measurements, Shiraiwa et al. (2007) derived the time scale from the increase of the fraction of coated particles with particle diameter twice its insoluble core (i.e., condensed secondary species represents 87.5% of the overall particle volume). In contrast, a coating of sulfate or nitrate corresponding to 16% of overall particle volume may be sufficient for non-hygroscopic particles to become CCN at atmospheric relevant supersaturation, and the aerosol can be treated as an internal mixture for the calculation of N_{CCN}. Riemer et al. (2004) defined the conversion of hydrophobic BC to hydrophilic particles as soluble species contributing to 5% of particle volume, and found the time scale is often less than 2 hours during daytime in polluted regions. The non-hygroscopic HOA and BC particles observed during night agree with earlier modeling studies that show much longer conversion time scales of 10 to 40 hrs during night (Riemer et al., 2004). During daytime, the thin coating required to increase the κ of non-hygroscopic particles to 0.1 and the rapid production of secondary hygroscopic species suggest except when freshly emitted (i.e. within a few hours) POA and BC represents a large fraction of total aerosol volume, N_{CCN} may be predicted using an internal mixture assumption to within 20%, and using bulk composition may be sufficient as shown by the results from T0 site.

As aerosols age, the production of secondary species, including sulfate, nitrate, and SOA, reduces the contribution of POA and BC to overall aerosol volume. As a result, the difference among N_{CCN} calculated assuming different mixing states may be quite small for aged aerosols, such as those observed from 10:00 to 16:00 at T0 site during MILAGRO. This suggests that while physically unrealistic, external mixtures, which are used in many global models, may also predict N_{CCN} with sufficient accuracy for aged aerosols, because non-hygroscopic POA and BC are quickly overwhelmed in particle volume by the condensation of secondary species (e.g. Volkamer et al., 2006; de Gouw and Jimenez, 2009; DeCarlo et al., 2010) and often contribute a small fraction of the total aerosol volume (Sciare et al., 2005; Williams et al., 2007; Zhang et al., 2007; Aggarwal et al., 2009; Jimenez et al., 2009). This finding is also consistent with the result from an earlier study (Ervens et al., 2010).

6 Summary

Strong diurnal variations of aerosol properties were observed at the urban T0 site on weekdays during MILAGRO. High number concentrations of Aitken mode particles and elevated mass concentrations of POA and BC observed during morning hours are attributed to traffic emissions. Measurements from the TDMA indicate that during 06:00–08:00, freshly emitted BC and POA were mostly externally mixed with other hygroscopic species. Starting from ∼07:30 substantial increases in nitrate and O+BBOA concentrations were observed. In a few hours from 09:00 to 12:00, HOA and BC particles, initially externally-mixed from the accumulation mode aerosol, were quickly mixed with secondary nitrate and SOA, and became hygroscopic. CCN concentrations are derived using measured aerosol size distributions, size-resolved chemical composition, and mixing state inferred from TDMA measurements, and agree with concurrent measurements at five supersaturations ranging from 0.11 to 0.35%.

Sensitivity analyses using measurements during MILAGRO and representative aerosol types suggest that mixing state strongly influences the calculated N_{CCN} only when weak or non-hygroscopic species (i.e., $\kappa < 0.1$) contribute a substantial fraction ($> \sim 50\%$) of the aerosol volume. As SOA and BBOA typically have κ values of ∼0.1 or greater, this suggests that assumed mixing state strongly impacts calculated N_{CCN} only when POA and BC represent a large fraction of the total aerosol volume, such as the aerosols observed during morning traffic hours at the T0 site, when POA and BC contributed to 52% of the total aerosol volume. A much reduced difference among N_{CCN} calculated using different mixing states is found during 10:00–16:00, when HOA and BC only presented 23% of the total aerosol volume.

The analyses also indicate that, while ambient particles may exhibit a wide spectrum of composition at a given size, if great majority of particles has an overall κ value greater than 0.1, N_{CCN} may be derived within 20% assuming an internal mixture (i.e., at any size, particles are mixtures of all participating species and have the identical composition). This uncertainty corresponds to less than ∼10% in the uncertainty of derived droplet number concentration (Sotiropoulou et al., 2006). Increasing the κ of a non-hygroscopic particle from 0 to 0.1 corresponds to condensed sulfate (or nitrate) representing 16% of the overall particle volume. For a non-hygroscopic particle of 100 nm in diameter, this translates into a 3 nm sulfate coating. The measurements at T0 site suggest that during daytime, the mixing of POA and BC particles with hygroscopic species and the increase of their κ to 0.1 takes place in a few hours, representing a substantially shorter photochemical time scale for converting hydrophobic particles into hydrophilic ones than the 1–2 days used in many global models (Wilson et al., 2001; Chung and Seinfeld, 2002). The results from T0 site also indicate more homogeneous particle composition among different particle sizes following the condensation of secondary species. This rapid process suggests that during daytime, a few tens of kilometers away from HOA and BC sources, N_{CCN} may be derived (within ∼20%) by assuming an internal mixture and using bulk chemical composition. The mixing time scale is substantially longer during night. Most HOA and BC particles emitted during evening traffic hours likely remain non-hygroscopic until efficiently mixed with photochemically produced hygroscopic species the next morning.

As aerosols age, the production of secondary species such as sulfate, nitrate, and SOA reduces the contribution of POA and BC to the overall aerosol volume, and thereby the impact of assumed aerosol mixing state on calculated N_{CCN}. In aged aerosols, most species are internally mixed to some degree. One implication of the above results is that while physically unrealistic, external mixtures, which are used in many global models, may also accurately predict N_{CCN} for aged aerosols, as the contribution of non-hygroscopic HOA and BC to overall aerosol volume is often small due to the condensation of secondary species.

Acknowledgements. The authors thank Jeffrey Gaffney and Nancy Marley for providing aethalometer data, and Robert Osborn and Runjun Li for their assistance of operating SMPS and CCN counter at the T0 site. We acknowledge Mexican Institute of Petroleum for hosting the T0 supersite, and logistics support from Molina Center for Energy and the Environment, Mexican government agencies, and institutions. This work was supported by the US Department of Energy's Atmospheric Science Program (Office of Science, OBER) under contract DE-AC02-98CH10886. MJC, ACA, and JLJ's contribution was supported by DOE DE-FG02-05ER63981 and DEFG0208ER64627, NSF ATM-0449815, and NOAA NA08OAR4310565.

Edited by: L. Molina

References

Aggarwal, S. G. and Kawamura, K.: Carbonaceous and inorganic composition in long-range transported aerosols over northern Japan: Implication for aging of water-soluble organic fraction, Atmos. Environ., 43, 2532–2540, 2009.

Aiken,A. C., DeCarlo, P. F., Kroll, J. H., et al.: O/C and OM/OC Ratios of Primary, Secondary, and Ambient Organic Aerosols with High Resolution Time-of-Flight Aerosol Mass Spectrometry Environ. Sci. Technol., 42, 4478–4485, 2008.

Aiken, A. C., Salcedo, D., Cubison, M. J., Huffman, J. A., DeCarlo, P. F., Ulbrich, I. M., Docherty, K. S., Sueper, D., Kimmel, J. R., Worsnop, D. R., Trimborn, A., Northway, M., Stone, E. A., Schauer, J. J., Volkamer, R. M., Fortner, E., de Foy, B., Wang, J., Laskin, A., Shutthanandan, V., Zheng, J., Zhang, R., Gaffney, J., Marley, N. A., Paredes-Miranda, G., Arnott, W. P., Molina, L. T., Sosa, G., and Jimenez, J. L.: Mexico City aerosol analysis during MILAGRO using high resolution aerosol mass spectrometry at the urban supersite (T0) - Part 1: Fine particle composition and organic source apportionment, Atmos. Chem. Phys., 9, 6633–6653, doi:10.5194/acp-9-6633-2009, 2009.

Aiken, A. C., de Foy, B., Wiedinmyer, C., et al.: Mexico City aerosol analysis during MILAGRO using high resolution aerosol mass spectrometry at the urban supersite (T0) – Part 2: Analysis of the biomass burning contribution and the modern carbon fraction, Atmos. Chem. Phys., 10, 5315–5341, 2010, http://www.atmos-chem-phys.net/10/5315/2010/.

Albrecht, B. A.: Aerosols, cloud microphysics, and fractional cloudiness, Science, 245, 1227–1230, 1989.

Andreae, M. O. and Rosenfeld, D.: Aerosol-cloud-precipitation interactions. Part 1. The nature and sources of cloud-active aerosols, Earth Sci. Rev., 89, 13–41, 2008.

Asa-Awuku, A., Engelhart, G. J., Lee, B. H., Pandis, S. N., and Nenes, A.: Relating CCN activity, volatility, and droplet growth kinetics of beta-caryophyllene secondary organic aerosol, Atmos. Chem. Phys., 9, 795–812, doi:10.5194/acp-9-795-2009, 2009.

Bergin, M. H., Schwartz, S. E., Halthore, R. N., et al.: Comparison of aerosol optical depth inferred from surface measurements with that determined by Sun photometry for cloud-free conditions at a continental US site, J. Geophys. Res., 105, 6807–6816, 2000.

Bilde, M. and Svenningsson, B.: CCN activation of slightly soluble organics: the importance of small amounts of inorganic salt and particle phase, Tellus B, 56, 128–134, 2004.

Broekhuizen, K., Chang, R. Y. W., Leaitch, W. R., Li, S. M., and Abbatt, J. P. D.: Closure between measured and modeled cloud condensation nuclei (CCN) using size-resolved aerosol compositions in downtown Toronto, Atmos. Chem. Phys., 6, 2513–2524, doi:10.5194/acp-6-2513-2006, 2006.

Canagaratna, M. R., Jayne, J. T., Jimenez, J. L., et al.: Chemical and Microphysical Characterization of Ambient Aerosols with the Aerodyne Aerosol Mass Spectrometer, Mass Spec. Rev., 26, 185–222, 2007.

Cantrell, W., Shaw, G., Cass, G. R., et al.: Closure between aerosol particles and cloud condensation nuclei at Kaashidhoo Climate Observatory, J. Geophys. Res., 106, 28711–28718, 2001.

Cappa, C. D. and Jimenez, J. L.: Quantitative estimates of the volatility of ambient organic aerosol, Atmos. Chem. Phys., 10, 5409–5424, doi:10.5194/acp-10-5409-2010, 2010.

Carrico, C. M., Petters, M. D., Kreidenweis, S. M., et al.: Aerosol hygroscopicity and cloud droplet activation of extracts of filters from biomass burning experiments, J. Geophys. Res., 113, D08206, doi: 10.1029/2007JD009274, 2008.

Chang, R. Y. W., Liu, P. S. K., Leaitch, W. R., and Abbatt, J. P. D.: Comparison between measured and predicted CCN concentrations at Egbert, Ontario: Focus on the organic aerosol fraction at a semi-rural site, Atmos. Environ., 41, 8172–8182, 2007.

Chung, S. H. and Seinfeld, J. H.: Global distribution and climate forcing of carbonaceous aerosols, J. Geophys. Res., 107, 4407, doi:10.1029/2001JD001397, 2002.

Clegg, S. L., Brimblecombe, P., and Wexler, A. S.: Thermodynamic model of the system H^+-NH_4^+-Na^+-SO_4^{2-}-$NB_{3\_}$-Cl^--H_2O at 298.15 K, J. Phys. Chem. A, 102, 2155–2171, 1998.

Collins, D. R., Flagan, R. C., and Seinfeld, J. H.: Improved inversion of scanning DMA data, Aerosol Sci. Technol., 36, 1–9, 2002.

Conant, W. C., VanReken, T. M., Rissman, T. A., et al.: Aerosol-Cloud Drop Concentration Closure in Warm Cumulus. J. Geophys. Res., 109, D13204, doi:10.1029/2003JD004324, 2004.

Cross, E. S., Slowik, J. G., Davidovits, P., et al.: Laboratory and ambient particle density determinations using light scattering in conjunction with aerosol mass spectrometry, Aerosol Sci. Tech., 41, 343–359, 2007.

Cross, E. S., Onasch, T. B., Canagaratna, M., Jayne, J. T., Kimmel, J., Yu, X.-Y., Alexander, M. L., Worsnop, D. R., and Davidovits, P.: Single particle characterization using a light scattering module coupled to a time-of-flight aerosol mass spectrometer, Atmos. Chem. Phys., 9, 7769–7793, doi:10.5194/acp-9-7769-2009, 2009.

Cubison, M. J., Ervens, B., Feingold, G., Docherty, K. S., Ulbrich, I. M., Shields, L., Prather, K., Hering, S., and Jimenez, J. L.: The influence of chemical composition and mixing state of Los Angeles urban aerosol on CCN number and cloud properties, Atmos. Chem. Phys., 8, 5649–5667, doi:10.5194/acp-8-5649-2008, 2008.

DeCarlo, P., Slowik, J. G., Worsnop, D. R., et al.: Particle Morphology and Density Characterization by Combined Mobility and Aerodynamic Diameter Measurements. Part 1: Theory. Aerosol Sci. Technol., 38, 1185–1205, 2004.

DeCarlo, P. F., Kimmel, J. R., Trimborn, A., et al.: Field-Deployable, High-Resolution, Time-of-Flight Aerosol Mass Spectrometer, Anal. Chem., 78, 8281–8289, 2006.

de Gouw, J. and Jimenez, J. L.: Organic Aerosols in the Earth's Atmosphere. Environ. Sci. Technol., 43, 7614–7618, 2009.

Dusek, U., Frank, G. P., Hildebrandt, L., et al.: Size matters more than chemistry for cloud-nucleating ability of aerosol particles, Science, 312, 1375–1378, 2006.

Dzepina, K., Volkamer, R. M., Madronich, S., Tulet, P., Ulbrich, I. M., Zhang, Q., Cappa, C. D., Ziemann, P. J., and Jimenez, J. L.: Evaluation of Recently-Proposed Secondary Organic Aerosol Models for a Case Study in Mexico City, Atmos. Chem. Phys., 9, 5681–5709, doi:10.5194/acp-9-5681-2009, 2009.

Easter, R. C., Ghan, S. J., Zhang, Y., et al.: MIRAGE: Model description and evaluation of aerosols and trace gases, J. Geophys. Res., 109, D20210, doi:10.1029/2004JD004571, 2004.

Ervens, B., Cubison, M., Andrews, E., et al.: Prediction of cloud condensation nucleus number concentration using measurements of aerosol size distributions and composition and light scattering enhancement due to humidity, J. Geophys. Res., 112, D10S32, doi:10.1029/2006JD007426, 2007.

Ervens, B., Cubison, M. J., Andrews, E., Feingold, G., Ogren, J. A., Jimenez, J. L., Quinn, P. K., Bates, T. S., Wang, J., Zhang, Q., Coe, H., Flynn, M., and Allan, J. D.: CCN predictions using simplified assumptions of organic aerosol composition and mixing state: a synthesis from six different locations, Atmos. Chem. Phys., 10, 4795–4807, doi:10.5194/acp-10-4795-2010, 2010.

Facchini, M. C., Mircea, M., Fuzzi, S., and Charlson, R. J.: Cloud albedo enhancement by surface-active organic solutes in growing droplets, Nature, 401, 257–259, 1999.

Gasparini, R., Li, R. J., and Collins, D. R.: Integration of size distributions and size-resolved hygroscopicity measured during the Houston Supersite for compositional categorization of the aerosol, Atmos. Environ., 38, 3285–3303, 2004.

Gasparini, R., Li, R. J., Collins, D. R., et al.: Application of aerosol hygroscopicity measured at the Atmospheric Radiation Measurement Program's Southern Great Plains site to examine composition and evolution, J. Geophys. Res., 111, D05S12, doi:10.1029/2004JD005448, 2006.

Gong, S. L., Barrie, L. A., Blanchet, J. P., et al.: Cana-

dian Aerosol Module: A size-segregated simulation of atmospheric aerosol processes for climate and air quality models – 1. Module development, J. Geophys. Res., 108, 4007, doi:10.1029/2001JD002002, 2003.

Gunthe, S. S., King, S. M., Rose, D., Chen, Q., Roldin, P., Farmer, D. K., Jimenez, J. L., Artaxo, P., Andreae, M. O., Martin, S. T., and Poschl, U.: Cloud condensation nuclei in pristine tropical rainforest air of Amazonia: size-resolved measurements and modeling of atmospheric aerosol composition and CCN activity, Atmos. Chem. Phys., 9, 7551–7575, doi:10.5194/acp-9-7551-2009, 2009.

Huff-Hartz, K. E. H., Tischuk, J. E., Chan, M. N., et al.: Cloud condensation nuclei activation of limited solubility organic aerosol, Atmos. Environ., 40, 605–617, 2006.

Huffman, J. A., Docherty, K. S., Aiken, A. C., et al: Chemically-resolved aerosol volatility measurements from two megacity field studies, Atmos. Chem. Phys., 9, 7161–7182, doi:10.5194/acp-9-7161-2009, 2009.

Intergovernmental panel on Climate Change (IPCC): Climate change 2007: The physical science basis, Cambridge University Press, New York, USA, 2007.

Jimenez, J. L., Canagaratna, M. R., Donahue, et al.: Evolution of Organic Aerosols in the Atmosphere, Science, 326, 1525–1529, 2009.

Johnson, K. S., Zuberi, B., Molina, L. T., Molina, M. J., Iedema, M. J., Cowin, J. P., Gaspar, D. J., Wang, C., and Laskin, A.: Processing of soot in an urban environment: case study from the Mexico City Metropolitan Area, Atmos. Chem. Phys., 5, 3033–3043, doi:10.5194/acp-5-3033-2005, 2005.

Kanakidou, M., Seinfeld, J. H., Pandis, S. N., Barnes, I., Dentener, F. J., Facchini, M. C., Van Dingenen, R., Ervens, B., Nenes, A., Nielsen, C. J., Swietlicki, E., Putaud, J. P., Balkanski, Y., Fuzzi, S., Horth, J., Moortgat, G. K., Winterhalter, R., Myhre, C. E. L., Tsigaridis, K., Vignati, E., Stephanou, E. G., and Wilson, J.: Organic aerosol and global climatemodelling: a review, Atmos. Chem. Phys., 5, 1053–1123, doi:10.5194/acp-5-1053-2005, 2005.

King, S. M., Rosenoern, T., Shilling, J. E., et al.: Cloud condensation nucleus activity of secondary organic aerosol particles mixed with sulfate, Geophys. Res. Lett., 34, L24806, doi: 10.1029/2007GL030390, 2007.

King, S. M., Rosenoern, T., Shilling, J. E., Chen, Q., and Martin, S. T.: Increased cloud activation potential of secondary organic aerosol for atmospheric mass loadings, Atmos. Chem. Phys., 9, 2959–2971, doi:10.5194/acp-9-2959-2009, 2009.

Köhler, H.: The nucleus in and the growth of hygroscopic droplets, Trans. Farad. Soc., 32, 1152–1161, 1936.

Liu, P. S. K., Leaitch, W. R., Banic, C. M., et al.: Aerosol observations at Chebogue Point during the 1993 North Atlantic Regional Experiment: Relationships among cloud condensation nuclei, size distribution, and chemistry, J. Geophys. Res., 101, 28971–28990, 1996.

Malloy, Q. G. J., Nakao, S., Qi, L., et al.: Real-Time Aerosol Density Determination Utilizing a Modified Scanning Mobility Particle SizerAerosol Particle Mass Analyzer System, Aerosol Sci. Tech., 43, 673–678, 2009.

Marley, N. A., Gaffney, J. S., Castro, T., Salcido, A., and Frederick, J.: Measurements of aerosol absorption and scattering in the Mexico City Metropolitan Area during the MILAGRO field campaign: a comparison of results from the T0 and T1 sites, Atmos. Chem. Phys., 9, 189-206, 2009, http://www.atmos-chem-phys.net/9/189/2009/.

Medina, J., Nenes, A., Sotiropoulou, R. E. P., et al.: Cloud condensation nuclei closure during the International Consortium for Atmospheric Research on Transport and Transformation 2004 campaign: Effects of size-resolved composition, J. Geophys. Res., 112, D10S31, doi:10.1029/2006JD007588, 2007.

Ming, Y., Ramaswamy, V., Donner, L. J., et al.: Modeling the interactions between aerosols and liquid water clouds with a self-consistent cloud scheme in a general circulation model, J. Atmos. Sci., 64, 1189–1209, 2007.

Mircea, M., Facchini, M. C., Decesari, S., Cavalli, F., Emblico, L., Fuzzi, S., Vestin, A., Rissler, J., Swietlicki, E., Frank, G., Andreae, M. O., Maenhaut, W., Rudich, Y., and Artaxo, P.: Importance of the organic aerosol fraction for modeling aerosol hygroscopic growth and activation: a case study in the Amazon Basin, Atmos. Chem. Phys., 5, 3111–3126, doi:10.5194/acp-5-3111-2005, 2005.

Mochida, M., Kuwata, M., Miyakawa, T., et al.: Relationship between hygroscopicity and cloud condensation nuclei activity for urban aerosols in Tokyo, J. Geophys. Res., 111, D23204,, doi:10.1029/2005JD006980, 2006.

Moffet, R. C., de Foy, B., Molina, L. T., Molina, M. J., and Prather, K. A.: Measurement of ambient aerosols in northern Mexico City by single particle mass spectrometry, Atmos. Chem. Phys., 8, 4499–4516, doi:10.5194/acp-8-4499-2008, 2008.

Moffet, R. C. and Prather, K. A.: In-situ measurements of the mixing state and optical properties of soot with implications for radiative forcing estimates, Proc. Natl. Acad. Sci. USA, 106, 11872–11877, 2009.

Molina, L. T., Madronich, S., Gaffney, J. S., Apel, E., de Foy, B., Fast, J., Ferrare, R., Herndon, S., Jimenez, J. L., Lamb, B., Osornio-Vargas, A. R., Russell, P., Schauer, J. J., Stevens, P. S., and Zavala, M.: An overview of the MILAGRO 2006 campaign: Mexico City emissions and their transport and transformation, Atmos. Chem. Phys. Discuss., 10, 7819–7983, doi:10.5194/acpd-10-7819-2010, 2010.

Moteki, N., Kondo, Y., Miyazaki, Y., et al.: Evolution of mixing state of black carbon particles: Aircraft measurements over the western Pacific in March 2004, Geophys. Res. Lett., 34, L11803, doi: 10.1029/2006GL028943, 2007.

Murphy, D. M., Cziczo, D. J., Froyd, K. D., et al., Single-particle mass spectrometry of tropospheric aerosol particles, J. Geophys. Res., 111, D23S32, doi:10.1029/2006JD007340, 2006.

Paatero, P.: Least squares formulation of robust non-negative factor analysis, Chemom. Intell. Lab. Syst., 37, 23–35, 1997.

Paredes-Miranda, G., Arnott, W. P., Jimenez, J. L., Aiken, A. C., Gaffney, J. S., and Marley, N. A.: Primary and secondary contributions to aerosol light scattering and absorption in Mexico City during the MILAGRO 2006 campaign, Atmos. Chem. Phys., 9, 3721–3730, doi:10.5194/acp-9-3721-2009, 2009.

Park, K., Kittelson, D. B., Zachariah, M. R., and McMurry, P. H.: Measurement of inherent material density of nanoparticle agglomerates, J. Nanopart. Res., 6, 267–272, 2004.

Petters, M. D., and Kreidenweis, S. M.: A single parameter representation of hygroscopic growth and cloud condensation nucleus activity, Atmos. Chem. Phys., 7, 1961–1971, doi:10.5194/acp-7-1961-2007, 2007.

Petters, M. D., Carrico, C. M., Kreidenweis, S. M., et al.: Cloud condensation nucleation activity of biomass burning aerosol. J. Geophys. Res., 114, D22205, doi: 10.1029/2009JD012353, 2009.

Prenni, A. J., Petters, M. D., Kreidenweis, S. M., et al.: Cloud droplet activation of secondary organic aerosol, J. Geophys. Res., 112, D10223, doi:10.1029/2006JD007963, 2007.

Quinn, P. K., Bates, T. S., Coffman, D. J., and Covert, D. S.: Influence of particle size and chemistry on the cloud nucleating properties of aerosols, Atmos. Chem. Phys., 8, 1029–1042, doi:10.5194/acp-8-1029-2008, 2008.

Raymond, T. M. and Pandis, S. N.: Cloud activation of single-component organic aerosol particles, J Geophys. Res., 107, 4787, doi:10.1029/2002JD002159, 2002.

Raymond, T. M. and Pandis, S. N.: Formation of cloud droplets by multicomponent organic particles, J Geophys. Res., 108, 4469, doi:10.1029/2003JD003503, 2003.

Riemer, N., Vogel, H., and Vogel, B.: Soot aging time scales in polluted regions during day and night, Atmos. Chem. Phys., 4, 1885–1893, doi:10.5194/acp-4-1885-2004, 2004.

Riemer, N., West, M., Zaveri, R. A., and Easter, R. C.: Simulating the evolution of soot mixing state with a particle-resolved aerosol model, J. Geophys. Res., 114, D09202, doi:10.1029/2008JD011073, 2009.

Rissler, J., Swietlicki, E., Zhou, J., Roberts, G., Andreae, M. O., Gatti, L. V., and Artaxo, P.: Physical properties of the sub-micrometer aerosol over the Amazon rain forest during the wet-to-dry season transition – comparison of modeled and measured CCN concentrations, Atmos. Chem. Phys., 4, 2119–2143, doi:10.5194/acp-4-2119-2004, 2004.

Roberts, G. C., Artaxo, P., Zhou, J. C., et al.: Sensitivity of CCN spectra on chemical and physical properties of aerosol: A case study from the Amazon Basin, J Geophys. Res., 107, 8070, doi:10.1029/2001JD000583, 2002.

Roberts, G. C. and Nenes, A.: A continuous-flow streamwise thermal-gradient CCN chamber for atmospheric measurements, Aerosol Sci. Technol., 39, 206–221, 2005.

Rose, D., Nowak, A., Achtert, P., Wiedensohler, A., Hu, M., Shao, M., Zhang, Y., Andreae, M. O., and Pschl, U.: Cloud condensation nuclei in polluted air and biomass burning smoke near the mega-city Guangzhou, China – Part 1: Size-resolved measurements and implications for the modeling of aerosol particle hygroscopicity and CCN activity, Atmos. Chem. Phys., 10, 3365-3383, doi:10.5194/acp-10-3365-2010, 2010.

Rose, D., Gunthe, S. S., Mikhailov, E., Frank, G. P., Dusek, U., Andreae, M. O., and Pöschl, U.: Calibration and measurement uncertainties of a continuous-flow cloud condensation nuclei counter (DMT-CCNC): CCN activation of ammonium sulfate and sodium chloride aerosol particles in theory and experiment, Atmos. Chem. Phys., 8, 1153–1179, doi:10.5194/acp-8-1153-2008, 2008.

Salcedo, D., Onasch, T. B., Dzepina, K., et al.: Characterization of ambient aerosols in Mexico City during the MCMA-2003 campaign with Aerosol Mass Spectrometry: results from the CENICA Supersite, Atmos. Chem. Phys., 6, 925–946, doi:10.5194/acp-6-925-2006, 2006.

Salcedo, D., Onasch, T. B., Aiken, A. C., et al: Determination of particulate lead during MILAGRO/MCMA-2006 using Aerosol Mass Spectrometry, Atmos. Chem. Phys., 10, 5371–5389, 2010, http://www.atmos-chem-phys.net/10/5371/2010/. doi:10.5194/acp-10-5371-2010, 2010.

Sciare, J., Oikonomou, K., Cachier, H., Mihalopoulos, N., Andreae, M. O., Maenhaut, W., and Sarda-Esteve, R.: Aerosol mass closure and reconstruction of the light scattering coefficient over the Eastern Mediterranean Sea during the MINOS campaign, Atmos. Chem. Phys., 5, 2253–2265, doi:10.5194/acp-5-2253-2005, 2005.

Seinfeld, J. H. and Pandis, S. N.: Atmospheric Chemistry and Physics, 2nd ed., John Wiley & Sons, Inc., Hoboken, p. 371, 2006.

Shinozuka, Y., Clarke, A. D., DeCarlo, P. F., Jimenez, J. L., Dunlea, E. J., Roberts, G. C., Tomlinson, J. M., Collins, D. R., Howell, S. G., Kapustin, V. N., McNaughton, C. S., and Zhou, J.: Aerosol optical properties relevant to regional remote sensing of CCN activity and links to their organic mass fraction: airborne observations over Central Mexico and the US West Coast during MILAGRO/INTEX-B, Atmos. Chem. Phys., 9, 6727–6742, doi:10.5194/acp-9-6727-2009, 2009.

Shiraiwa, M., Kondo, Y., Moteki, N., et al.: Evolution of mixing state of black carbon in polluted air from Tokyo, Geophys. Res. Lett., 34, L16803, doi:10.1029/2007GL029819, 2007.

Shulman, M. L., Jacobson, M. C., Carlson, R. J., et al.: Dissolution behavior and surface tension effects of organic compounds in nucleating cloud droplets, Geophys. Res. Lett., 23, 277–280, 1996.

Sotiropoulou, R. E. P., Medina, J., and Nenes, A.: CCN predictions: Is theory sufficient for assessments of the indirect effect? Geophys. Res. Lett., 33, L05816, doi:10.1029/2005GL025148, 2006.

Stroud, C. A., Nenes, A., Jimenez, J. L., et al.: Cloud activating properties of aerosol observed during CELTIC, J. Atmos. Sci., 64, 441–459, 2007.

Svenningsson, B., Rissler, J., Swietlicki, E., Mircea, M., Bilde, M., Facchini, M. C., Decesari, S., Fuzzi, S., Zhou, J., Monster, J., and Rosenorn, T.: Hygroscopic growth and critical supersaturations for mixed aerosol particles of inorganic and organic compounds of atmospheric relevance, Atmos. Chem. Phys., 6, 1937–1952, doi:10.5194/acp-6-1937-2006, 2006.

Textor, C., Schulz, M., Guibert, S., Kinne, S., Balkanski, Y., Bauer, S., Berntsen, T., Berglen, T., Boucher, O., Chin, M., Dentener, F., Diehl, T., Easter, R., Feichter, H., Fillmore, D., Ghan, S., Ginoux, P., Gong, S., Kristjansson, J. E., Krol, M., Lauer, A., Lamarque, J. F., Liu, X., Montanaro, V., Myhre, G., Penner, J., Pitari, G., Reddy, S., Seland, O., Stier, P., Takemura, T., and Tie, X.: Analysis and quantification of the diversities of aerosol life cycles within AeroCom, Atmos. Chem. Phys., 6, 1777-1813, doi:10.5194/acp-6-1777-2006, 2006.

Turpin, B. J. and Lim, H. J.: Species contributions to PM2.5 mass concentrations: Revisiting common assumptions for estimating organic mass, Aerosol Sci. Technol., 35, 602–610, 2001.

Twomey, S.: Influence of Pollution on Shortwave Albedo of Clouds, J. Atmos. Sci., 34, 1149–1152, 1977.

Ulbrich, I. M., Canagaratna, M. R., Zhang, Q., Worsnop, D. R., and Jimenez, J. L.: Interpretation of organic components from Positive Matrix Factorization of aerosol mass spectrometric data, Atmos. Chem. Phys., 9, 2891–2918, doi:10.5194/acp-9-2891-2009, 2009.

VanReken, T. M., Rissman, T. A., Roberts, G. C., et

al.: Toward aerosol/cloud condensation nuclei (CCN) closure during CRYSTAL-FACE, J Geophys. Res., 108, 4633, doi:10.1029/2003JD003582, 2003.

Velasco, E., Pressley, S., Grivicke, R., Allwine, E., Coons, T., Foster, W., Jobson, B. T., Westberg, H., Ramos, R., Hernández, F., Molina, L. T., and Lamb, B.: Eddy covariance flux measurements of pollutant gases in urban Mexico City, Atmos. Chem. Phys., 9, 7325–7342, doi:10.5194/acp-9-7325-2009, 2009.

Vestin, A., Rissler, J., Swietlicki, E., et al.: Cloud-nucleating properties of the Amazonian biomass burning aerosol: Cloud condensation nuclei measurements and modeling, J. Geophys. Res., 112, D14201, doi:10.1029/2006JD8104, 2007.

Volkamer, R., Jimenez, J. L., San Martini, F., et al.: Secondary Organic Aerosol Formation from Anthropogenic Air Pollution: Rapid and Higher than Expected. Geophys. Res. Lett., 33, L17811, doi:10.1029/2006GL026899, 2006.

Wang, J., Flagan, R. C., and Seinfeld, J. H.: A differential mobility analyzer (DMA) system for submicron aerosol measurements at ambient relative humidity, Aerosol Sci. Technol., 37, 46–52, 2003.

Wang, J., Lee, Y. N., Daum, P. H., Jayne, J., and Alexander, M. L.: Effects of aerosol organics on cloud condensation nucleus (CCN) concentration and first indirect aerosol effect, Atmos. Chem. Phys., 8, 6325–6339, doi:10.5194/acp-8-6325-2009, 2008.

Williams, B. J., Goldstein, A. H., Millet, et al.: Chemical speciation of organic aerosol during the International Consortium for Atmospheric Research on Transport and Transformation 2004: Results from in situ measurements, J. Geophys. Res., 112, D10S26, doi:10.1029/2006JD007601, 2007.

Wilson, J., Cuvelier, C., and Raes, F.: A modeling study of global mixed aerosol fields, J. Geophys. Res., 106, 34081–34108, 2001.

Zhang, Q., Worsnop, D. R., Canagaratna, M. R., and Jimenez, J. L.: Hydrocarbon-like and oxygenated organic aerosols in Pittsburgh: insights into sources and processes of organic aerosols, Atmos. Chem. Phys., 5, 3289–3311, doi:10.5194/acp-5-3289-2005, 2005a.

Zhang, Q., Canagaratna, M. R., Jayne, J. T., et al.: Time and Size-Resolved Chemical Composition of Submicron Particles in Pittsburgh – Implications for Aerosol Sources and Processes. J. Geophys. Res., 110, D07S09, doi:10.1029/2004JD004649, 2005b.

Zhang, Q., Jimenez, J. L., Canagaratna, M. R., et al: Ubiquity and dominance of oxygenated species in organic aerosols in anthropogenically-influenced Northern Hemisphere midlatitudes, Geophys. Res. Lett., 34, L13801, doi:10.1029/2007GL029979, 2007.